A Current-Mode Potentiostat for Multi-Target Detection Tested with Different Lactate Biosensors

S. Sara Ghoreishizadeh, Irene Taurino, Sandro Carrara*, and Giovanni De Micheli
EPFL, LSI - Lausanne - Switzerland
*sandro.carrara@epfl.ch

***Abstract*—Real-time and multi-target detection by wireless implantable devices is of increasing interest for chronic patients. In this work, electrode sharing is proposed to minimize the size of the implantable device when several three-electrode-based sensing sites are needed. An integrated potentiostat and readout circuit for a multi-target biosensor is presented. To realize this, the circuit reads out the sensor current through each working electrode in a current-mode scheme. The maximum detectable current is 8 μA and the simulated input referred current noise of the circuit is 125 pA/$\sqrt{\text{Hz}}$ at 1 Hz. The circuit was fabricated in 0.18 μm technology and tested for two lactate biosensors fabricated with a commercial lactate oxidase and an engineered one. Chronoamperometry experiments performed with the circuit agree well with a commercial equipment for lactate detection up to 1 mM.**

***Index Terms*—Multi-target biosensor, Potentiostat, Readout circuit, Integrated circuit, Chronoamperometry, Lactate.**

I. Introduction

The development of new implantable devices for wireless and real-time monitoring of human metabolic conditions is of great importance in case of chronic diseases. In this context, detection of more than one biomolecule such as glucose, lactate, and ATP is an urgent need and it can be achieved by the use of multi-target biosensors. A multi-target biosensor consists of several sensing sites, each dedicated to the detection of a single marker compound. The most common structure of the sensing site has three electrodes: *working electrode* (WE), *counter electrode* (CE) and *reference electrode* (RE) [1]. To decrease the size of a multi-target biosensor, CE and RE can be shared among all the WEs. Each WE can specifically detect one metabolite of interest thanks to an electrochemical reaction that takes place at a given voltage. The potentiostat is a circuit that keeps this voltage on the sensing site. Several potentiostats and readout circuits have been designed for a three-electrode based biosensor in [2] [3] [4] [5] for single target detection. The common feature, is the readout through the CE. However, in biosensors with several sensing sites that share CE and RE, the current through CE is the sum of the currents from all different sensing sites. Therefore, it can not be used to measure the current of a specific sensing site. Other works like [6] [7] present integrated potentiostats with current readout through the WE, but for single target detection via a two-electrode based biosensor.

In this work, we propose a readout and potentiostat circuit for *chronoamperometry* (CA) measurements via multi-target three-electrode biosensors with WEs sharing the same CE and RE. The circuit fixes a voltage at the WE and reads the relative current. The accuracy of the voltage at the WE and also noise of the circuit is studied. Finally, the circuit has been electrically and electrochemically tested with two L-lactate sensors. Indeed, L-lactate is one of the major biocompound of health interest. Examples of amperometric biosensors of L-lactate are described by applying *L-lactate* oxidase (LODx) from various sources [8]. These biosensors use only natural enzymes and suffer from the lack of sufficient stability/functionality to be used for viable devices. On the other hand, the design of adequate proteins allows the enhancement of the sensing performance [9]. All the sensor parameters are also strongly influenced by the immobilization method of the enzyme onto the electrode. In this work we utilize one relatively new and promising approach, which has been established for a variety of enzyme based sensors. The approach is to immobilize enzymes on *multi-walled carbon nanotubes* (MWCNTs) by a simple physical adsorption [10]. MWCNT is promising nanomaterial in electrochemical sector because of the excellent conducting properties [11]. Moreover, carbon nanotubes preserve the enzyme activity once adsorbed onto the top of their surface [12].

The CMOS circuit for multi-target biosensor is presented in Section II; The noise of the circuit and the error on the WE voltage are analysed in this section; Section III presents the measurement method and results on two MWCNT-sensors based on a commercial and on an engineered LODx by using the integrated circuit.

II. Circuit Architecture

The circuit is depicted in Fig. 1. It consists of two operational amplifiers and two current mirrors. OP_1 is a folded cascode design with an NMOS input stage. OP_2 is also folded cascode with a dual n- and p-MOS input stage. OP_1 and the electrochemical cell create a negative feedback through which RE voltage is set to V_{RE}. OP_1 also provides current to CE.

OP_2 and MP_0 create another negative feedback that fixes the voltage of the selected WE at V_{WE}. The current of the sensor in the oxidation mode flows from the WE to the CE and is provided by the MP_0 and MP_2. A copy of this current is provided by MP_3 and MP_1 to be used for the readout instead of using the sensor current. To provide more isolation for the sensor from the next circuit block that can be an ADC [2] [3], the copied current is mirrored again using MN_2 and MN_3. The gain of the current mirrors is set to 1 to decrease power

consumption. The current is finally converted to voltage by the resistor R. We refer to this part of the circuit (OP_2, the current mirrors, and the resistor R) as the readout core. The mutual transimpedance gain of the readout core is therefore equal to the resistor R if we assume the output resistance of the NMOS current mirror to be very high.

In Fig. 1, a multiplexer is used to connect the readout core to one sensing site at a time. The circuit can also be employed for a simultaneous measurement of current from multiple sensing sites, if we simply repeat the readout core and connect each of them to one sensing site, without multiplexing.

The two main reasons why current readout from CE is usually preferred to WE in the literature are: (1) The WE voltage should remain constant regardless of the current; (2) Connecting the WE to a constant voltage, results in less noise compared to connecting it to any circuit [3]. We will focus on these properties of the circuit, namely the error in the WE voltage and the equivalent current noise in the WE.

A. WE voltage error evaluation

To find the error in V_{WE} with respect to the negative terminal of OP_2 we derive the transfer function using the small signal model of the transistors. The transfer function is:

$$\frac{V_{WE}}{V_{neg,OP2}} = \frac{1}{1 - \frac{g_{m,MP0} + g_{m,MP2}}{Z \times A \times g_{m,MP0} \times g_{m,MP2}}} \quad (1)$$

where Z is the equivalent impedance seen from the WE to the ground and its typical value in low frequency is few hundreds of $k\Omega$. A is the gain of the amplifier OP_2, which is 70 dB and g_m is the transconductance of the transistors which highly depends on the biosensor current. Eq. 1 shows that the error is directly proportional to the sum of transconductances of MP_2 and MP_0 and inversely proportional to their product. Therefore, to decrease the error in the voltage of the WE, both $g_{m,MP0}$ and $g_{m,MP2}$ are designed to be high and equal by choosing a high $\frac{W}{L}$ ratio. The error introduced by the multiplexer can be also reduced adequately by increasing the $\frac{W}{L}$ ratio of the switches.

B. Noise analysis

Fig. 2 shows the main noise sources in the implemented circuit and the sensor. These are the noise of the current mirrors, OP_1, and the noise of the biosensor which is related to the electrochemical reactions and the thermal noise coming from the inherent resistance of electrodes and solution. Since the spectral components of the current are at low frequencies, only the low frequency component of the noise is of interest. At low frequencies the contribution of the cascade MOSFETs to the total noise is negligible [13]. The same reasoning holds true for the noise of the multiplexer. The input-referred current noise of the system at a selected WE is equal to:

$$I^2_{n,in} = I^2_{n,snsr.} + I^2_{n,OP1} + I^2_{n,MP2} + \frac{1}{4}(I^2_{n,MP1} + g^2_{m,MP1} V^2_{n,OP2}) + (\frac{g_{m,MP2}}{g_{m,MP3}})^2 \times [I^2_{n,MN2} + I^2_{n,MP3} + (I^2_{n,MN3} + I^2_{n,R}) \times (\frac{g_{m,MN2}}{g_{m,MN3}})^2] \quad (2)$$

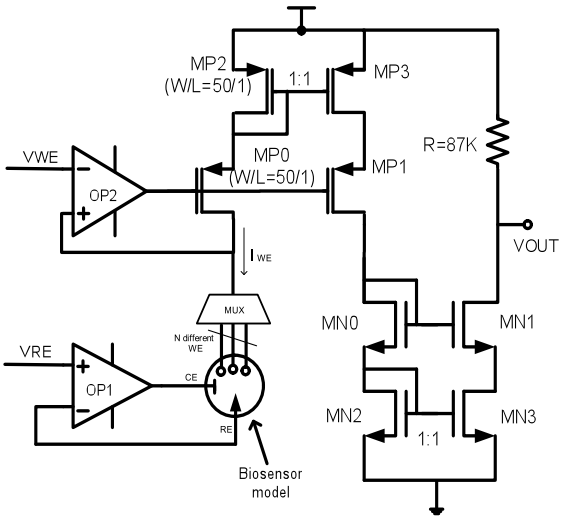

Fig. 1. Schematic of the circuit.

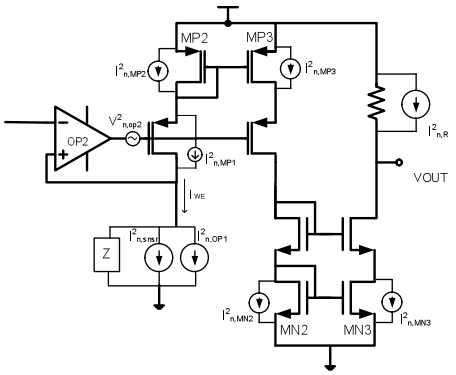

Fig. 2. Main noise sources of the circuit.

where $g_{m,MNx}$ and $g_{m,MPy}$ are the transconductances of MNx and the MPy transistors, respectively. In the circuit the gain of both current mirrors is equal to one and the dimensions of all NMOS transistors and all PMOS transistors are the same. Therefore, we can assume that the transconductance and the noise of all NMOS and all PMOS transistors are equal. Then Eq. 2 can be rewritten as:

$$I^2_{n,in} = I^2_{n,snsr} + I^2_{n,OP1} + \frac{1}{4} g^2_{m,MP1} V^2_{n,OP2} + 2.25 I^2_{n,MP2} + 2 I^2_{n,MN2} + I^2_{n,R} \quad (3)$$

where

$$I^2_{n,R} = \frac{4KT}{R} \quad (4)$$

$$I^2_{n,MX2} = 4\gamma KT g_{m,MX2} + \frac{K_f}{C_{ox} f} \times \frac{g^2_{m,MX2}}{(WL)_{MX2}} \quad (5)$$

where K, T, and γ are Boltzmann constant, absolute temperature and a technology dependent coefficient, respectively. C_{ox} is the gate oxide capacitance, f is the frequency and K_f is the flicker noise constant. According to Eq. 4 and 5, to reduce the equivalent input noise of the circuit, g_m of the NMOS and PMOS transistors should be minimized and the area of the transistors should be maximized. This means to increase the

transistor width and length at the same time. On the other hand, to decrease the input referred current noise of the circuit, the output resistance should be maximized as well. The resistance R is determined by the required readout circuit gain. The use of a higher resistance can be compensated by reducing the current mirrors gain to achieve the same readout gain. However, this strategy increases the input-referred noise according to Eq. 2. The simulated input-referred current noise of the whole circuit is 125 pA/$\sqrt{\text{Hz}}$ at 1 Hz.

C. Electrical measurements

The circuit was fabricated in 0.18 μm CMOS technology. To eliminate errors due to mismatches and process variation, all matched components in the design of the current mirrors were kept as symmetrical as possible by using either a one-dimensional or a full two-dimensional common-centroid design. The area of the circuit is 0.009 mm^2. The measured transimpedance of the circuit is 86.5$\pm$ 0.2 kΩ. The error is computed from four series of measurements. An example of the input-output characteristics of the circuit is shown in Fig. 3. It is measured using the RC equivalent of the biosensor in the top site of Fig. 3.

III. Electrochemical measurements

The circuit is used to measure L-lactate concentrations with two LODx-MWCNT-sensors. Sensor preparation, measurement methods and results are presented in the following subsections.

A. Chemicals and electrode preparation

Carboxyl group (-COOH) functionalized MWCNTs with a diameter of 10 nm and a length of 1-2 μm were purchased from DropSens (Spain) in form of a powder (90% purity). MWCNTs were diluted in chloroform with a final concentration equal to 1 mg/ml [10]. Before doing the experiments, all solutions were sonicated to guarantee homogeneity. The electrochemical behavior of two LODxs from *Aerococcus viridans* adsorbed onto the MWCNT-electrode surfaces was studied: a commercial enzyme (cLODx) from Roche (10 kU/120 mg; dilution: *phosphate buffered saline* (PBS) 10 mM, pH 7.4) and a wild type (wtLODx) from EPMA (St. Gallen, Swizerland; concentration: 0.03173 mg/ml; activity: 117 U/ml;

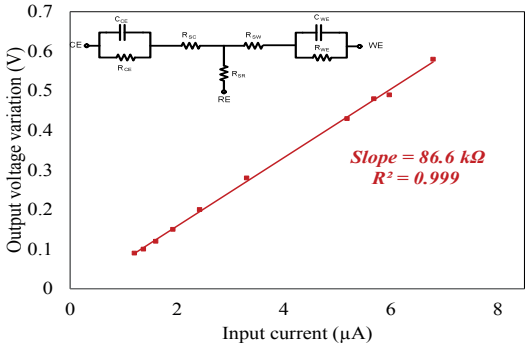

Fig. 3. The measured transimpedance gain of the fabricated circuit. Top side: RC model of one sensing side used to measure the gain of the circuit.

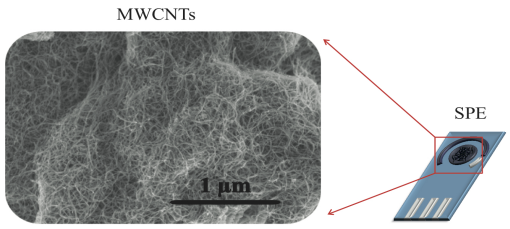

Fig. 4. SEM image of MWCNTs immobilized onto graphite SPE.

dilution: PBS 200 mM, pH 7.0). Lithium L-lactate in form of lyophilized powder (Sigma, Switzerland) was dissolved in Milli-Q water. *Screen-printed electrodes* (SPEs) were obtained from DropSens (model DRP-110). The working electrode was made in graphite with an active area equal to 12.54 mm^2. The counter electrode was also in graphite and the reference was an Ag|AgCl electrode. MWCNT-chloroform solution (30 μl) was deposited by drop casting (5 μl portions) onto the working electrodes [14]. The chloroform was allowed to evaporate between two subsequent deposition steps [14]. The enzymes (26 μg per each type) were additionally cast onto the nanostructured working electrodes. Fig. 4 shows a SEM image of MWCNTs cast onto a the WE of a SPE.

B. Electrochemical apparatus

The electrochemical response was investigated by CA at room temperature under aerobic conditions. Routinely, the electrodes were dipped into a 25 ml stirred PBS solution (10 mM pH 7.4). The concentration was varied by steps of 0.2 mM by adding successively 10 μl of 0.5 M L-lactate solution. The time-step depended on the current stabilization.

Fig 5 shows the experimental set-up we used to measure L-lactate with our circuit. A commercial potentiostat, namely Versastat 3 potentiostat from Princeton Applied Technologies, is also used for the measurements of L-lactate by using the same modified SPEs for comparison purpose.

C. Measurement results

The electrochemical behavior of MWCNT-SPEs based on cLODx and wtLODx was studied with both the fabricated integrated circuit and the commercial potentiostat. In both cases the sensor was kept under the fixed voltage equal to +650 mV (for the proposed circuit by applying $V_{WE} = 1.35V$ and $V_{RE} = 0.7V$) until the stabilization of the current.

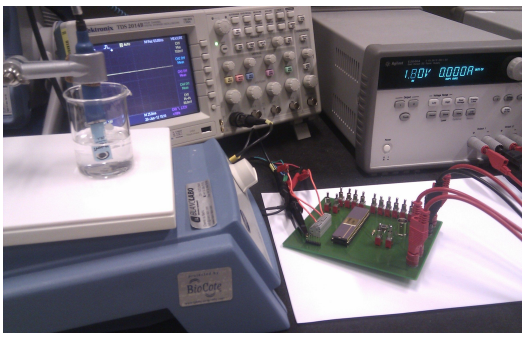

Fig. 5. Set-up for lactate measurement with the fabricated integrated circuit.

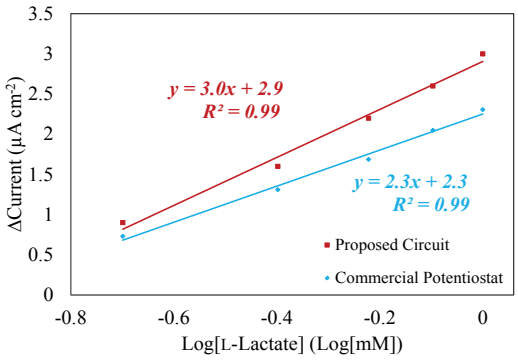

Fig. 6. The measured calibration curves acquired with the circuit and with a commercial potentiostat by using SPEs-based on cLODx.

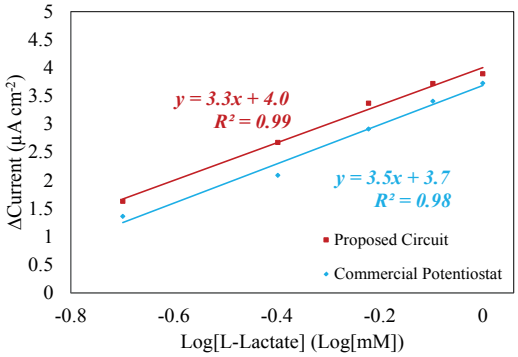

Fig. 7. The measured calibration curves acquired with the circuit and with a commercial potentiostat by using SPEs-based on the wtLODx.

A stable sensor should have a current smaller that 500 nA in absence of the L-lactate (i.e. zero concentration) [15]. Having a stable sensor, the measurement was performed as explained in Section III-B. Sensitivity per unit of area was computed from the slope of the straight line obtained by plotting the steady-state current per electrode area versus the L-lactate concentration in the range of linearity [16]. Fig. 6 and 7 show the calibration curves obtained from CAs and related to measurements with cLODx and wtLODx-based SPEs, respectively. The vertical axis shows the current of the sensor, which is acquired using the characteristics in Fig. 3 for the measurements by our proposed circuit it. By using both the commercial instrument and our circuit the values of sensitivities and linear ranges related to each LODx-based sensor are similar (linear regression equations and related R^2 in Fig. 6 and 7).

IV. Conclusions

A current-mode potentiostat and readout circuit is presented for multi-target detection using multiple sensing sites with shared CE and RE and independent and different WEs. The circuit was fabricated in 0.18 μm technology. It occupies 0.009 mm^2 and consumes 80 μW from 1.8 V supply voltage, which is suitable for implantable applications[17]. It is shown that the provided WE voltage is highly controllable. The circuit is used to characterize two L-lactate bisensors based on two different L-lactate oxidises, wtLODx and cLODx. CA measurement results using the fabricated circuit agree well with the commercial equipment.

V. Acknowledgment

The authors would like to thank Linda Thöny-Meyer for providing wtLODx and Fabienne Bobard for acquisition of the SEM image. The research has been funded by the project i-IronIC that is financed with a grant from the Swiss Nano-Tera.ch initiative and evaluated by the Swiss National Science Foundation. This work is also supported in part by the NanoSys project (program ERC-2009-AdG-246810).

References

[1] A. J. Bard and L. R. Faulkner, *Electrochemical methods : fundamentals and applications*. Wiley, New York, 1980.

[2] M. Haider, S. Islam, S. Mostafa, M. Zhang, and T. Oh, "Low-power low-voltage current readout circuit for inductively powered implant system," *Biomedical Circuits and Systems, IEEE Transactions on*, vol. 4, no. 4, pp. 205 –213, 2010.

[3] M. Ahmadi and G. Jullien, "Current-mirror-based potentiostats for three-electrode amperometric electrochemical sensors," *Circuits and Systems I: Regular Papers, IEEE Transactions on*, vol. 56, no. 7, pp. 1339 –1348, 2009.

[4] P.-A. Boutet and S. Manen, "Low power cmos potentiostat for three electrodes amperometric chemical sensor," in *Faible Tension Faible Consommation (FTFC), 2011*, 2011, pp. 15 –18.

[5] Y.-T. Liao, H. Yao, A. Lingley, B. Parviz, and B. Otis, "A 3- cmos glucose sensor for wireless contact-lens tear glucose monitoring," *Solid-State Circuits, IEEE Journal of*, vol. 47, no. 1, pp. 335 –344, 2012.

[6] R. Genov, M. Stanacevic, M. Naware, G. Cauwenberghs, and N. Thakor, "16-channel integrated potentiostat for distributed neurochemical sensing," *Circuits and Systems I: Regular Papers, IEEE Transactions on*, vol. 53, no. 11, pp. 2371 –2376, 2006.

[7] M. Nazari and R. Genov, "A fully differential cmos potentiostat," in *Circuits and Systems, 2009. ISCAS 2009. IEEE International Symposium on*, 2009, pp. 2177 –2180.

[8] Z. Bori, G. Csiffáry, D. Virág, M. Tóth-Markus, A. Kiss, and N. Adányi, "Determination of l-lactic acid content in foods by enzyme-based amperometric bioreactor," *Electroanalysis*, vol. 24, no. 1, pp. 158–164, 2012.

[9] K. Sode, T. Ootera, M. Shirahane, A. Witarto, S. Igarashi, and H. Yoshida, "Increasing the thermal stability of the water-soluble pyrroloquinoline quinone glucose dehydrogenase by single amino acid replacement," *Enzyme and microbial technology*, vol. 26, no. 7, pp. 491–496, 2000.

[10] S. Carrara, V. Shumyantseva, A. Archakov, and B. Samorì, "Screen-printed electrodes based on carbon nanotubes and cytochrome P450scc for highly sensitive cholesterol biosensors," *Biosensors and Bioelectronics*, vol. 24, no. 1, pp. 148–150, 2008.

[11] K. Balasubramanian and M. Burghard, "Biosensors based on carbon nanotubes," *Analytical and bioanalytical chemistry*, vol. 385, no. 3, pp. 452–468, 2006.

[12] W. Feng and P. Ji, "Enzymes immobilized on carbon nanotubes," *Biotechnology advances*, 2011.

[13] B. Razavi, *Design of Analog CMOS Integrated Circuits*. McGraw-Hill, 2000.

[14] C. Boero, S. Carrara, G. Vecchio, L. Calzà, and G. Micheli, "Highly sensitive carbon nanotube-based sensing for lactate and glucose monitoring in cell culture," *NanoBioscience, IEEE Transactions on*, vol. 10, no. 1, pp. 59–67, 2011.

[15] J. Wang, *Analytical electrochemistry*. Vch Verlagsgesellschaft Mbh, 2006.

[16] D. Thévenot, K. Toth, R. Durst, and G. Wilson, "Electrochemical biosensors: recommended definitions and classification," *Biosensors and Bioelectronics*, vol. 16, no. 1, pp. 121–131, 2001.

[17] J. Olivo, S. Carrara, and G. De Micheli, "Energy harvesting and remote powering for implantable biosensors," *Sensors Journal, IEEE*, vol. 11, no. 7, pp. 1573 –1586, 2011.